

**ANNUAL PROGRESS REPORT**

**1997 - 1998**

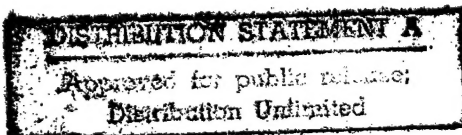
**INVESTIGATION OF A NEW CLASS OF LOW-PROFILE  
MULTI-LAYER PRINTED ANTENNAS**

**PRINCIPAL INVESTIGATOR:  
AHMAD HOORFAR, Ph.D.**



**DEPARTMENT OF ELECTRICAL AND  
COMPUTER ENGINEERING  
VILLANOVA UNIVERSITY  
VILLANOVA, PA 19085**

**PREPARED FOR:  
OFFICE OF NAVAL RESEARCH  
ARLINGTON, VA 22217**



**OCTOBER, 1998**

19981026 031

# INVESTIGATION OF A NEW CLASS OF LOW-PROFILE MULTI-LAYER PRINTED ANTENNAS

PERIOD: 10/97 - 9/98

PRINCIPAL INVESTIGATOR: AHMAD HOORFAR

## ABSTRACT

*This progress report outlines our research efforts on modeling, analyses and optimization of a novel class of multi-layered printed antennas for high gain applications. The proposed antennas, which are based on a multi-layer printed-circuit version of the conventional Yagi array, are very attractive for applications that require high gain antennas in a compact low-profile package. Presence of the dielectric layers not only hinders the need for structural support of the antenna but also provides a few more degrees of freedom for gain optimization. In addition, these antennas can be made conformal to various shapes and surfaces. Our research during this interim period has resulted in three contributions: 1) We have developed a numerical code for efficient electromagnetic modeling of these Yagi-like structures. A novel feature of this code is a new semi-analytical technique that speeds up the evaluation of the corresponding Green's functions by a factor of 10 or higher. 2) The feasibility of obtaining high gain from the proposed Yagi-like arrays is investigated by performing a detailed parametric study for structures with up to 5 dielectric layers. 3) We have developed an electromagnetic optimization engine based on Evolutionary Programming. This code is applied to optimal design of the printed Yagi-like arrays. Optimization is performed with respect to lengths of driver and director elements as well as dielectric constants and thickness of layers under different constraints' criteria. It is shown that a globally optimized three layer structures can achieve a gain of 13 dBi or higher without the need for high permittivity dielectric layers.*

# TABLE OF CONTENTS

<b>I. INTRODUCTION.....</b>	<b>4</b>
A. Objectives of the Present Research .....	4
B. Organization of the Report.....	5
<b>II. ANALYSIS OF “YAGI-LIKE” PRINTED ARRAYS FOR HIGH GAIN .....</b>	<b>5</b>
APPLICATIONS.....	5
A. Proposed Structures.....	5
B. Development of an Electromagnetic Model for the Antenna Structures.....	6
B.1. A Semi-Analytical Method for the Evaluation of Green’s Functions.....	7
B.2. Moment Method Implementation .....	9
C. High Gain Conditions for a Printed Dipole in a Multi-Layer Medium .....	7
D. Results and Discussions .....	10
<b>III. GAIN OPTIMIZATION USING EVOLUTIONARY PROGRAMMING.....</b>	<b>15</b>
A. Evolutionary Programming .....	15
B. Implementation of EP for the Printed Yagi-Like Structure .....	16
C. Results and Discussions.....	17
<b>IV. FUTURE WORKS .....</b>	<b>20</b>
<b>APPENDIX A.....</b>	<b>22</b>
<b>REFERENCES.....</b>	<b>25</b>
<b>REPORT DOCUMENTATION PAGE (Form 298).....</b>	<b>26</b>

## I. INTRODUCTION

This project focuses on three research topics which are of interest in various antenna applications in communications and radar. The topics under investigations are : 1) Investigation of a class of "Yagi-like" multilayer printed arrays for high gain applications, 2) New design concepts for low-profile dual-band CP microstrip antenna elements, and 3) Performance Analysis of multi-layer printed antenna structures on a curved surface.

### A. Objectives of the Present Research

The objective in Topic 1 is an in-depth theoretical as well as experimental investigation of a novel concept based on a multi-layer printed-circuit version of the conventional Yagi array in air. This structure is very attractive for applications that require high gain antennas in a compact low-profile package. Presence of the dielectric layers not only hinders the need for structural support of the antenna but also provides a few more degrees of freedom for gain optimization. In Topic 2, the objective is to investigate a new class of dual-band CP microstrip antennas, which are proximity-fed in a multi-layer dielectric substrate. Due to their electromagnetic feeding scheme these antennas are expected to have low spurious radiation from feed structures and thus well-suited for array applications in GPS and satellite communications. In Topic 3, the objective is to analyze the radiation performance of printed antennas in a multi-layered curved substrate/ground-plane environment. In particular, the effect of cylindrical curvature on the performances of the antenna structures in Topics 1 and 2 as well as their RCS response will be analyzed.

The present report details the progress made on the research Topic 1 during the time-period, October 1997 - September 1998. The technical contributions made during this period include:

- i) A computer code for efficient electromagnetic modeling of printed Yagi-like antennas in a general multi-layered medium has been developed. A novel feature of this code is a new semi-analytical technique which speeds up the evaluation of the corresponding Green's functions by a factor of 10 or higher.
- ii) Feasibility of obtaining high gain from the proposed printed Yagi-like dipole arrays has been investigated by performing a detailed parametric study for structures with up to 5 dielectric layers.
- iii) An electromagnetic optimization engine based on Evolutionary Programming has been developed. This code has been applied to optimal design of the printed Yagi-like arrays. Optimization has been performed with respect to lengths of driver and director elements as well as dielectric constants and thickness of layers under different constraints' criteria.

## **B. Organization of the Report**

This progress report is organized as follows. Development of an efficient Moment Method based computer code for modeling of multi-layer printed antennas in a general magneto-dielectric substrate is described in sections II-A and II-B. The application of this code to study the feasibility of obtaining high gain from the proposed multi-layered Yagi-like array is presented in sections II-C and II-D. Development of an electromagnetic optimization engine based on Evolutionary Programming and its application to optimized design of the Yagi-like structure is discussed in section III. Finally, future research work planned for this project is presented in section IV.

## **II. ANALYSIS OF "YAGI-LIKE" PRINTED ARRAYS FOR HIGH GAIN APPLICATIONS**

### **A. Proposed Structures**

The proposed multi-layered printed antenna structures, shown in Figures 1 and 2, present a low-profile alternative to the conventional Yagi-Uda array of wire dipoles which are widely used in communications and radar for high-gain applications. Although the Yagi-array has a relatively simple structure made of thin-wire elements, its overall length could become very large for high gain and/or low-frequency applications mainly due to the large number of directors and the required spacing between the elements. In addition, a mast must be used to structurally support the array elements in air. The structure in Figures 1 is a multi-layer printed-circuit version of the Yagi array of wire dipoles in air. This structure consists of a reflector, a driver and a finite number of embedded director strip elements. An alternative structure, shown in Figure 2, is a microstrip version of the array in Figure 1 and has a ground-plane in place of the reflector element. These structures give more degrees of freedom (i.e., the dielectric constants of the layers) when optimizing their design. They can also be made conformal to various shapes and surfaces (e.g., missiles, aircraft, or other flying objects). In addition, unlike the gain-enhancement techniques reported for an embedded microstrip dipole [1,2], the proposed structures can achieve high gains without the need for very high permittivity dielectric layers.

The above concepts can also be extended to other patch geometry (rectangular, circular, etc.) and feed-mechanism (coaxial, microstrip-line, etc.) as shown in Figure 3. It may also be possible to design these "Yagi-Like" structures for applications (e.g., satcom) that require circular-polarization (CP), by using for the driver and director elements such structures as printed cross-dipoles, cross-fed patches, nearly square patches, slotted patches, etc. Finally, a phased array consisting of the proposed Yagi-like antenna elements may be formed for beam-steering purposes as depicted in Figure 4.

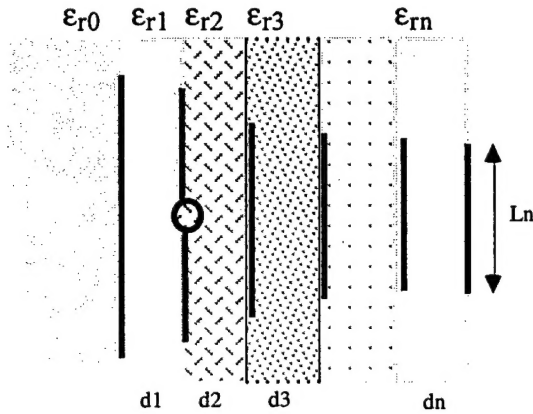


Figure 1: A printed Yagi-like dipole Array

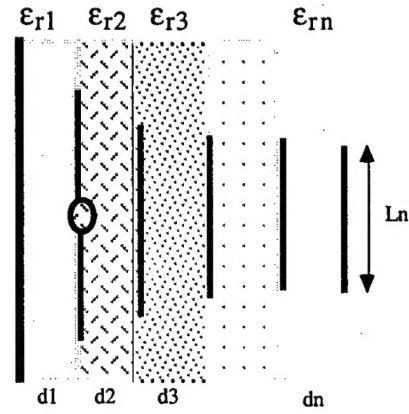


Figure 2: A Yagi stacked microstrip array in a multi-layered substrate

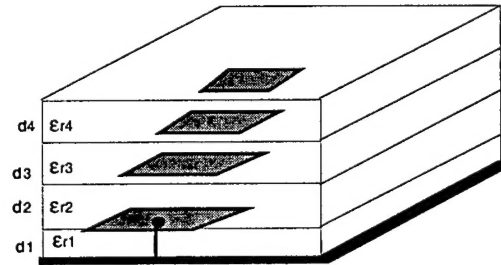


Figure 3: A coaxial-fed Yagi-like stacked microstrip patch array

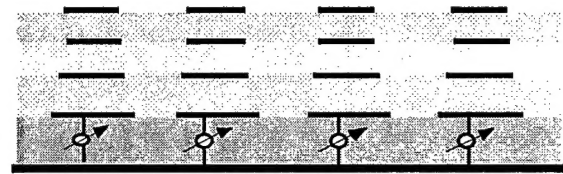


Figure 4: A phased-array of Yagi-like stacked patch sub-array elements

## B. Development of an Electromagnetic Model for the Antenna Structures

To optimize and design the proposed Yagi structures, an efficient numerical engine for accurate modeling of a general multi-layer printed antenna structure is needed. For the present problem the CPU efficiency of a numerical engine is of particular importance since one has to optimize the antenna gain with respect to the reflector, driver and directors lengths, thickness of the layers and their dielectric constants. A typical multi-parameter global optimization technique, may require the engine to be run hundreds of times in order to achieve a desired gain specification.

In this work, we have developed an efficient moment-method based technique that is well-suited for the present problem. The technique uses the so-called mixed-potential integral equation (MPIE)[3,4] which in general can model planar microstrip structure of arbitrary shape in a multi-layered medium (Figure 5). Our implementation of MPIE utilizes a newly developed technique for semi-analytical evaluation of the corresponding Green's functions and is, therefore, well suited for a medium with many dielectric layers.

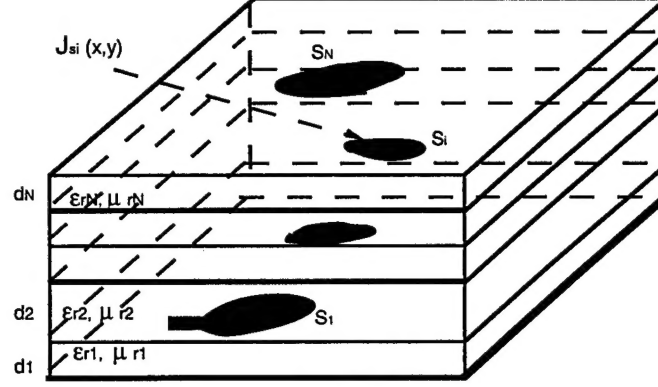


Figure 5: A multi-layered microstrip antenna structure

In general, the MPIE for a multi-layered structure can be written as:

$$\left( \frac{-j\eta_0 k_0^2}{2\pi} \right) \sum_{i=1}^N \iint_{S_i} \left[ G_{Mi}^{(p)}(\bar{x}, \bar{x}') \bar{J}_{si}(\bar{x}') + \frac{1}{k_0^2} \nabla_t G_{Ei}^{(p)}(\bar{x}, \bar{x}') \nabla_t' \cdot \bar{J}_{si}(\bar{x}') \right] dS_i' - Z_{sp} \bar{J}_{sp}(\bar{x}) = -\bar{E}_{inc}^{(p)} \quad (1)$$

$\bar{x} = (x, y) \in S ; p = 1, 2, \dots, N$

where  $J_{si}$  and  $Z_{si}$  are the electric surface current and the surface impedance of  $S_i$ , respectively;  $E_{inc}^{(p)}$  is the tangential (incident) electric field impressed at the  $p$ -th surface.  $G_{Mi}^{(p)}$  and  $G_{Ei}^{(p)}$  are the Green's Functions of Magnetic and Electric types, respectively, evaluated at the  $p$ -th layer due to a source at the  $i$ -th layer. The Green's functions are of the Sommerfeld integral type which can be expressed as the inverse Bessel transformation,

$$G_{E, M}(z, \rho) = 2\pi \int_0^\infty \tilde{G}_{E, M}(z, \lambda) J_0(k_0 \rho \lambda) \lambda d\lambda ; \quad \rho = \sqrt{(x-x')^2 + (y-y')^2} \quad (2)$$

(1)

where the spectral-domain Green's functions  $\tilde{G}_{E, M}(z, \lambda)$  satisfy the voltage distribution in an equivalent multi-section transmission line.

### B.1. A Semi-Analytical Method for the Evaluation of Green's Functions

In a typical moment method solution of the MPIE in (1), one has to numerically compute the spatial-domain Green's functions  $G_E$  and  $G_M$  in (2). The integral in (2), however, is of the Sommerfeld type which is not trivial to integrate due to its surface wave and branch-cut singularities. For an  $N$  layered structure with metalizations on all layers, there are  $M = 2 \sum_{m=1}^N (N - m + 1)$  unique Green's functions, requiring  $M$  numerical evaluations of the Sommerfeld

integral for each  $k_0\rho$  value, i.e., the normalized lateral distance between a source and an observation point. Each spectral-domain  $\tilde{G}$  has to be recursively determined from an equivalent multi-sectional transmission line representing the multi-layered medium. Since a large number of  $k_0\rho$  values are required, the CPU time spent on computation of the Green's functions can be prohibitively large when one attempts to develop a simulation / optimization program for the design of microstrip arrays located in such an environment.

In this work we have developed a semi-analytical method for evaluation of the Green's functions which significantly speeds up the numerical evaluation of these integrals. Here we briefly present an outline of the method. A more detailed formulation is presented in Appendix A. In this semi-analytical method we first deform a portion the contour of integration above the real-axis into the complex  $\lambda$  - plane, in order to avoid the singular behavior of the integrand near any surface wave poles, and then back to the real axis to infinity. Cubic-spline interpolations are used to curve-fit the spectral-domain integrand,  $\tilde{G}$ , in each region, except in the tail of the integrand, i.e.,  $\lambda_{\max}$  ( $\gg 1$ ) to infinity region, for which the integration range is divided into small pieces, using an adaptive marching scheme, and  $\tilde{G}$  is approximated on each piece by the first few terms in it's Taylor-series expansion in  $\lambda^{-2}$ . The resulting integrals can then be expressed in closed forms in terms of known special functions, namely, Bessel and Struve functions. These functions are of distance  $\rho$  only and independent of the dielectric layers' thickness and material properties. Therefore, once the constants in the cubic-spline interpolations and Taylor-series expansions are computed and stored, both the electric and magnetic type Green's functions can be evaluated for all values of  $\rho$  at once, resulting in a substantial reduction in the overall computation time. In addition, a scheme is developed in which the resulting special functions are computed only once for a given set of  $k_0\rho$  values, stored and then used for all  $M$  Green's functions of an  $N$ -layer structure. This results in an additional CPU time saving when metalized layers are present on two or more of the dielectric layers.

As an example, the Green's function  $G_e$  and  $G_m$  of a five layer structure are compared with the exact numerical integration in Figure 6. The results are shown for the case when the source and observation points are located on the 2nd and 3rd layers, respectively, The integral averaging technique [5] is used to speed up the numerical integration for the exact results. Excellent agreement for both the real-axis as well as the deformed complex parts of the contour are obtained. The normalized CPU time required for calculating all 30 distinct Green's functions of this five layer structure at 100  $k_0\rho$  points was only 10 seconds using the present method as compared to more than 220 seconds when the numerical integration was used. In general, as shown in Figure 7, the CPU time saving increases as the numbers of dielectric layers and the observation point



increase, indicating the efficiency of this method for antenna structures with a large number of conductors and dielectric layers.

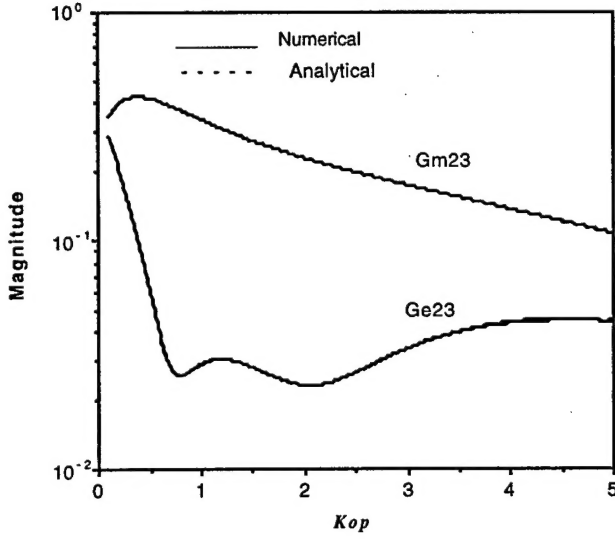


Figure 6: Results for the real-axis portion of the contour.  $\epsilon_{r1} = 2$ ,  $\epsilon_{r2} = 3$ ,  $\epsilon_{r3} = 4$ ,  $\epsilon_{r4} = 6$ ,  $\epsilon_{r5} = 2$ ;  $k_0d_1 = 0.1$ ,  $k_0d_2 = 0.1$ ,  $k_0d_3 = 0.05$ ,  $k_0d_4 = 0.1$ ,  $k_0d_5 = 0.2$ .

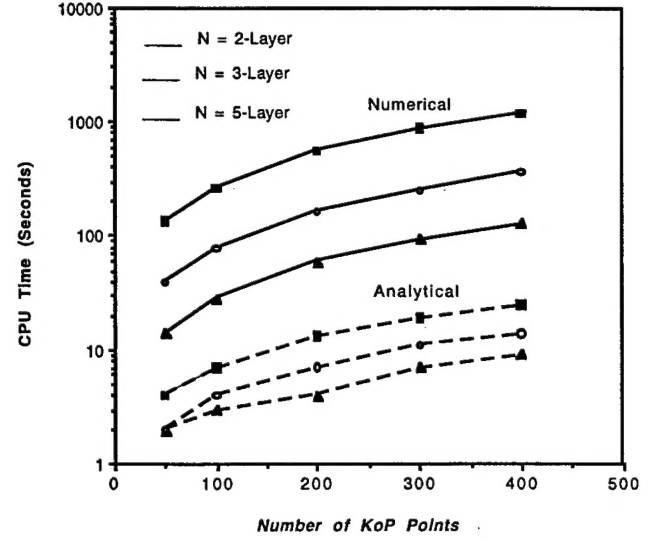


Figure 7: CPU time comparison between numerical and semi-analytical methods

## B.2. Moment Method Implementation

To solve the integral equation (1) numerically for the unknown current densities,  $J_{si}$ ,  $i=1,2,\dots,N$ , we have used a Galerkin/Moment Method solution. For the configurations in Figures 1 and 2 each strip conductor is assumed to have an electrically small width, thus the current on the strip is primarily flowing along its length, i.e., in the x-direction. Therefore, each dipole is divided into 20 rectangular cells per wavelength in x-direction and only 1 cell in y-direction. On each cell a constant basis function is used for the current. Constant basis functions are also used for the charge distribution,  $\nabla_t \cdot \bar{J}_s$ . The charge cells, however, are shifted by 1/2 cell with respect to the current cells in order to satisfy the continuity equation in an average sense.

## C. High Gain Conditions for a Printed Dipole in a Multi-Layer Medium

In order to understand the physics of radiation from printed Yagi-like antennas in Figures 1 and 2, we first need to examine the conditions of obtaining high gain from a printed dipole in the absence of any director elements. Let us consider a Hertzian dipole embedded in a multi-layered magneto-dielectric medium (see Figure 8). There are two types of high gain conditions for this

structure [2]. Type I condition requires that odd layers have high wave-impedance (i.e., large  $\mu_r$ ) , even layers have low-wave impedance (i.e., large  $\epsilon_r$ ) and

$$\frac{n_i d_i}{\lambda_0} = \frac{1}{2} , \quad \frac{n_i z_0}{\lambda_0} = \frac{1}{4} ; \quad \frac{n_i d_i}{\lambda_0} = \frac{1}{4} , \quad i \geq 2 \quad (3)$$

Type II condition requires that odd layers have low wave-impedance (i.e., large  $\epsilon_r$ ) , even layers have high wave-impedance (i.e., large  $\mu_r$ ) and

$$\frac{n_i d_i}{\lambda_0} = \frac{1}{4} , \quad \frac{n_i z_0}{\lambda_0} = \frac{1}{4} ; \quad \frac{n_i d_i}{\lambda_0} = \frac{1}{4} , \quad i \geq 2 \quad (4)$$

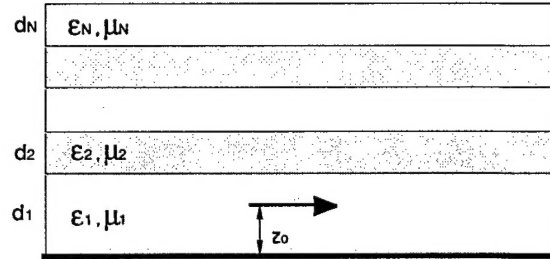


Figure 8: An embedded dipole in a multi-layered medium

where  $n_i = \sqrt{\epsilon_{ri} \mu_{ri}}$  is the refractive index of layer  $i$ . It is obvious that for a purely dielectric medium (i.e.  $\mu_r = 1$ ) , the dielectric layers should alternate between low and high permittivities. For example as shown in [6], for a resonant microstrip dipole in a two-layer medium with  $\epsilon_{r1} = 2$ , type I condition requires an  $\epsilon_{r2}$  of larger than 10 if a high gain of larger than 10 dBi together with high radiation efficiency (i.e., minimum of power lost to the surface-waves) is desired. This may not be feasible in practice because of the cost and heavy weight of high permittivity dielectric materials. As will be shown in the next section, introduction of director elements on the interfaces between dielectric layers resolves this problem.

#### D. Results and Discussions

A three layer “Yagi-like” stacked microstrip dipole array is shown in Figure 9. Figure 10 shows the gain of this structure plotted versus the director length ( $L_2 = L_3$ ) in  $\lambda_0$ , the free-space wavelength. All three layers are assumed to have  $\epsilon_{r1} = \epsilon_{r2} = \epsilon_{r3}$  and equal thickness,  $d_1 = d_2 = d_3 = 0.25 \lambda_d$ , where  $\lambda_d$  is the wavelength in dielectric. Width of each strip element is  $W = 0.021 \lambda_0$  and

the length of the driver is optimized for a resonance at the normalized frequency of  $f/f_0=1$ . As can be seen for  $\epsilon_r=2$  a gain of about 9.6 dBi is obtained when the each director has a length of about 0.32 free-space wavelength; the length of the driver in this case is  $L_1 = 0.302\lambda_0$ . We note that the same structure without the directors but with identical dielectric parameters has a gain of only about 5.84 dBi [6].

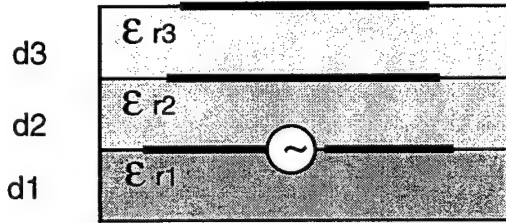


Figure 9: A three layer microstrip Yagi-like antenna

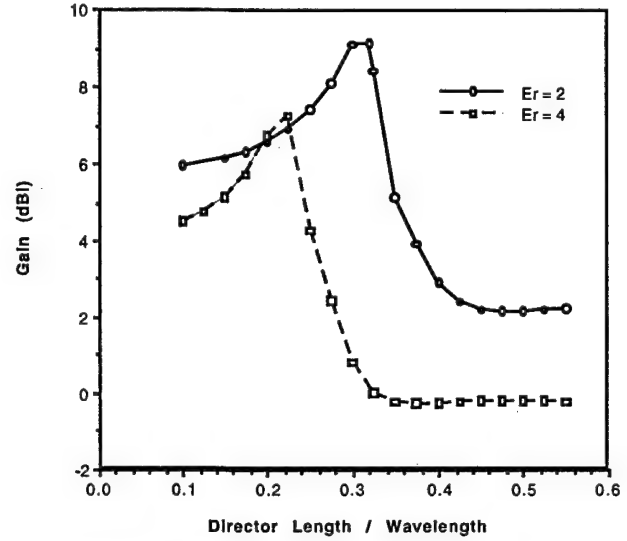


Figure 10: Gain of a printed 3-element stacked microstrip Yagi;  $\epsilon_{r1} = \epsilon_{r2} = \epsilon_{r3} = 2$  and 4;  $d_1 = d_2 = d_3 = 0.25 \lambda_d$

The Yagi-like structure can be further optimized and made more compact by keeping  $d_1$  fixed and varying  $d_2 = d_3$ , as shown in Figure 11. As seen, for  $d_2 = d_3 = 0.1 \lambda_d$  and  $\lambda_2 = \lambda_3 = 0.36 \lambda_0$ , a gain of about 10.1 dBi is obtained with an overall thickness of  $0.45 \lambda_d$  (nearly  $0.32 \lambda_0$ ). The corresponding driver's length is  $L_1 = 0.296 \lambda_0$ . The radiation efficiency (i.e., ratio of the radiated power to the total of the radiated plus the surface-wave powers) in this case is about 90% as compare to only about 67% for an embedded dipole case without the director elements. The Yagi-effect is in fact at work: addition of the two directors tends to focus the energy in the broadside direction and minimize the power lost to the surface-waves. Another evidence of this is the plot of the current distributions in Figure 12 where as seen a relatively substantial amount of current is induced on the director elements. The trade-off in this case is the gain bandwidth, which as shown in Figure 13, is much narrower for the Yagi-like structure than for the embedded dipole case without the director elements. In Figure 14, the gain versus the director length is shown for a structure with  $d_1 = 0.25 \lambda_{d1}$ ,  $\epsilon_{r1} = \epsilon_{r2} = 2$  and  $\epsilon_{r3} = 4$  and for various values of  $d_2/\lambda_{d2} = d_3/\lambda_{d3}$ .

Again, a high gain of more than 11 dBi is obtained when  $d_2/\lambda_{d2} = d_3/\lambda_{d3} = 0.235$  and  $L_2/\lambda_{d2} = L_3/\lambda_{d3} = 0.36$ . The corresponding resonant length of the driver in this case is about  $0.288\lambda_0$ . The same structure without the directors has a gain of only about 8 dBi. For this example the array gain decreases as values of  $d_2$  and  $d_3$  are further increased.

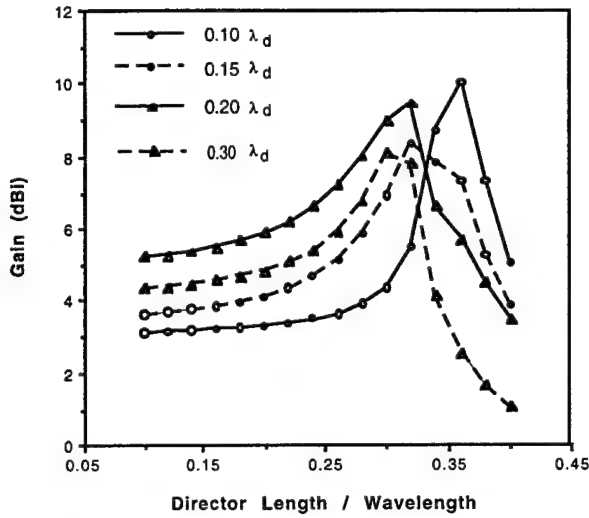


Figure 11: Gain of a printed 3-element stacked microstrip Yagi;  $\epsilon_{r1} = \epsilon_{r2} = \epsilon_{r3} = 2$ ,  $d_1 = 0.25 \lambda_d$

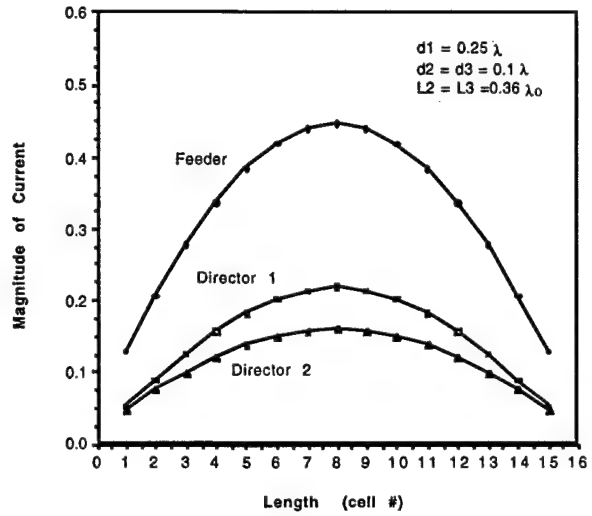


Figure 12: Current distributions on the stacked Yagi elements;  $\epsilon_{r1} = \epsilon_{r2} = \epsilon_{r3} = 2$ ,  $d_1 = 0.25 \lambda_d$

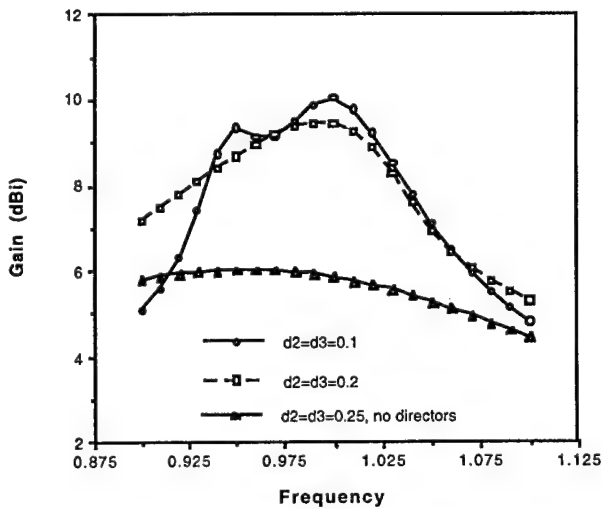


Figure 13: Gain of a 3-element stacked microstrip Yagi array as a function of normalized frequency.  $d_1 = 0.25 \lambda_d$

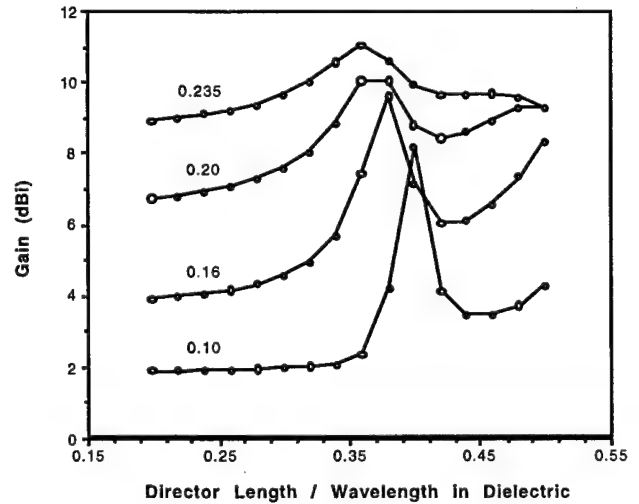


Figure 14: Gain of a 3-element stacked microstrip Yagi as a function of  $L_2/\lambda_{d2} = L_3/\lambda_{d3}$ ; The label on each curve is the ratio:  $d_2/\lambda_{d2} = d_3/\lambda_{d3}$ .

Higher gain values can be obtained by increasing the number of dielectric layers and combine the high gain condition discussed in section II.C (i.e., alternate between low and high  $\epsilon_r$ ) with the Yagi effect (i.e., directors at each interface). Figure 15 shows, the results for a five layer antenna with  $d_1 = 0.25 \lambda_{d1}$ ,  $\epsilon_{r1} = \epsilon_{r2} = \epsilon_{r4} = 2$ ,  $\epsilon_{r3} = \epsilon_{r5} = 4$  and for various values of  $d_2/\lambda_{d2} = d_3/\lambda_{d3} = d_4/\lambda_{d4} = d_5/\lambda_{d5}$ . Again, we have assumed all directors are of equal length. As can be seen, a high gain of more than 14 dBi is obtained when  $d_2/\lambda_{d2} = d_3/\lambda_{d3} = d_4/\lambda_{d4} = d_5/\lambda_{d5} = 0.245$ . An inspection of the current distributions for this case shows that the magnitude of the current on directors 1 and 3 are substantially more than those induced on the directors 2 and 4. It is noteworthy that directors 1 and 3 are at the transition interface between a low and a high permittivity layers, while directors 2 and 4 are at the interface between a high and a low permittivity layers. This phenomenon should be explored in more details in the future phases of this research since it may provide some guidelines for optimal design of these high gain antennas.

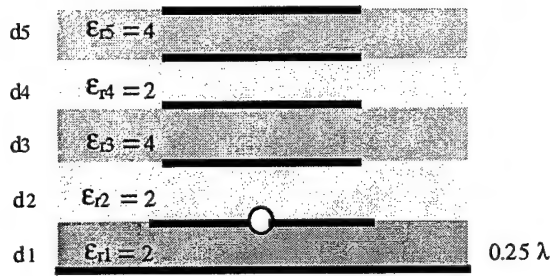
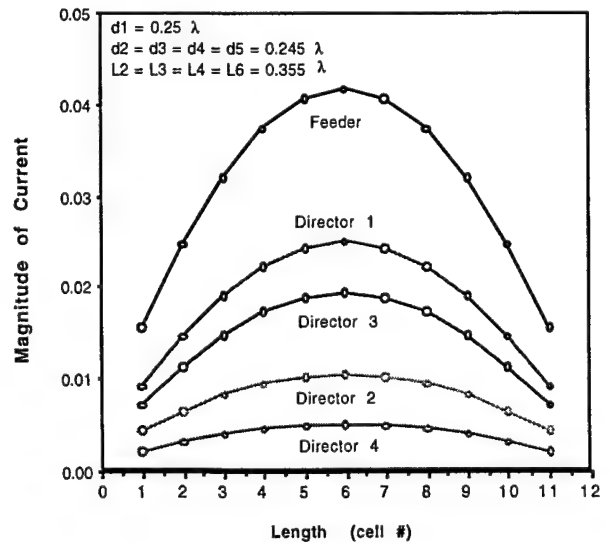
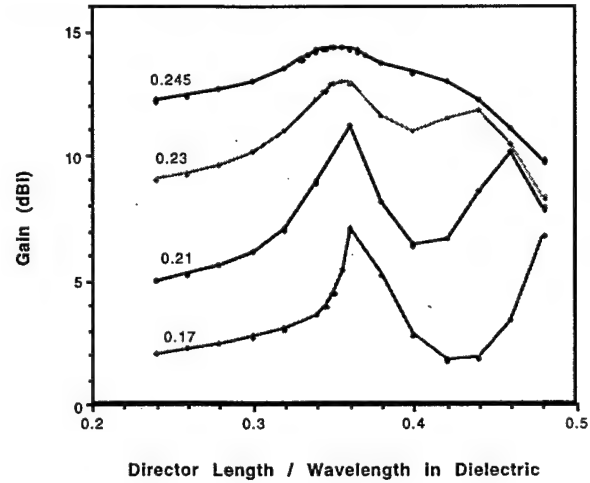


Figure 15: A five-layer microstrip Yagi-like antenna. Gain is plotted as a function of director length; the label on each curve is the ratio:  $d_2/\lambda_{d2} = d_3/\lambda_{d3} = d_4/\lambda_{d4} = d_5/\lambda_{d5}$ . Current distributions are plotted for the maximum gain case with  $d_2/\lambda_{d2} = d_3/\lambda_{d3} = d_4/\lambda_{d4} = d_5/\lambda_{d5} = 0.245$  and  $L_2/\lambda_{d2} = L_3/\lambda_{d3} = L_4/\lambda_{d4} = L_5/\lambda_{d5} = 0.355$ .



In all of the above examples the thickness of the first layer was assumed to be  $d_1/\lambda_{d1} = 0.25$ . The feeding mechanism in many microstrip patch antenna applications is coaxial or probe-fed which makes it undesirable to have a thick substrate thickness due to spurious radiation from the probe. As we have shown in Figure 16, however, it is possible to obtain a high gain even with an electrically thin substrate. For this case the frequency is 1 GHz and the substrate thickness is fixed at  $d_1 = 2.5$  mm. A gain of more than 11 dBi is obtained when  $d_2/\lambda_{d2} = d_3/\lambda_{d3} = 0.23$ .

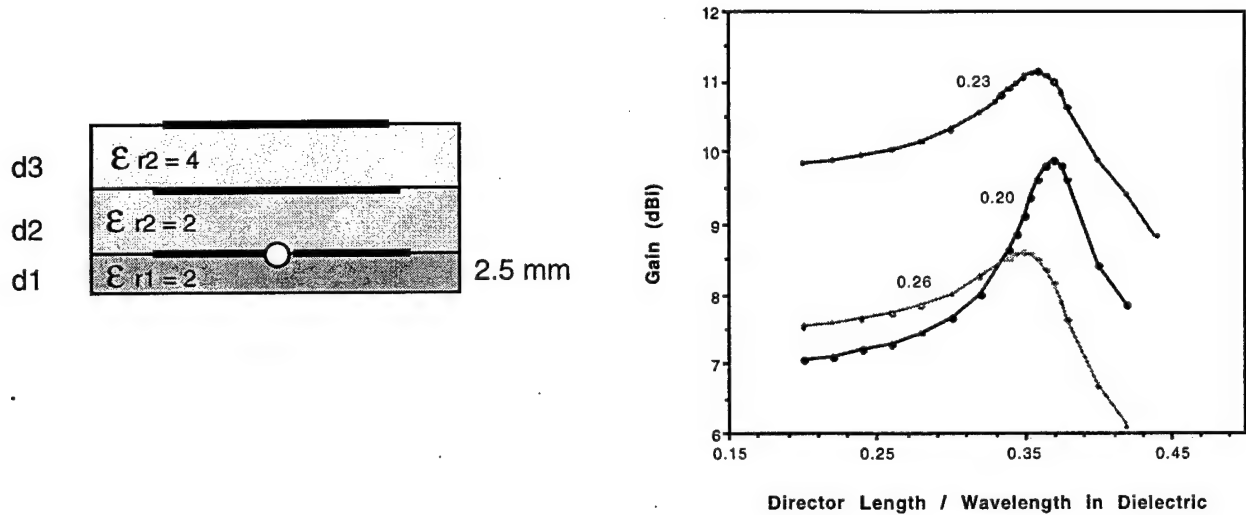


Figure 16: A three-layer microstrip Yagi with a thin substrate. Gain is plotted as a function of director length; the label on each curve is the ratio:  $d_2/\lambda_{d2} = d_3/\lambda_{d3}$ .

### III. GAIN OPTIMIZATION USING EVOLUTIONARY PROGRAMMING

The attempts outlined in section II-D to optimize the Yagi-like structure for high gain were arbitrary in nature and were done using a parametric study. Nevertheless, it was shown that a three layer structure with  $\epsilon_r = 2$  can produce a gain as high as 10 dBi or more, indicating its potential for high gains. Further, our investigation has indicated that the objective function relating the gain to the antenna parameters is highly non-linear and possesses multiple local optima. To successfully optimize this structure multi-parameter global optimization schemes, such as evolutionary algorithms, are necessary.

#### A. Evolutionary Programming

The evolutionary algorithms, such as genetic algorithms (GAs)[7], evolutionary programming (EP)[8], and evolutionary strategies (ES), are heuristic population-based search procedures that incorporate random variation and selection. Of the three paradigms GAs are well known to the electromagnetics community (see [9] for a detailed bibliography). Even though several successful applications have been reported, recent research has identified some inefficiencies in GA performance. This degradation in efficiency is apparent in applications with highly epistatic objective functions, i.e., where the parameters being optimized are highly correlated. On the other hand, EP and ES are more robust to epistatic objective functions and coordinate rotations. EP has been shown to be more efficient than GA on many function optimization problems [8].

The dynamics of GA have been explained through the building block hypothesis and the schema theorem [7], which are not fully accepted in the evolutionary computation literature. On the other hand, the convergence theory for EP is well established and EP has been proven to asymptotically converge to the global optimum with probability one, under elitist selection [8]. Further, EP is well suited for optimizing continuous, discrete, and mixed parameter optimization problems. Binary GAs require the parameters to be coded as bits; this could limit the accuracy of the solutions obtained. Further, the selection of the crossover and mutation probabilities is quite arbitrary and they are not adapted during evolution. The selection of the initial values for the strategy parameters for EP and ES are well defined and efficient adaptive and self-adaptive techniques exist for adapting these parameters during evolution.

The algorithm for a standard EP consists of seven general steps:

1. Initialization: Initialize parents uniformly over the population size of  $N$ .
2. Fitness Evaluation of Parents: evaluate the objective function for each parent.
3. Mutation: From each parent a single offspring is generated by adding a Gaussian random variable with the standard deviations, SD.

4. Fitness Evaluation of Offspring: evaluate the objective function for each offspring; The parents and offsprings constitute the new population.
5. Tournament: each solution competes against  $M$  ( $< N$ ) randomly chosen opponents and the number of wins for each solution is obtained.
6. Selection: the solutions with the greatest number of wins are selected to be the parents of the next generation.
7. Termination: is the best parent satisfactory? If yes, terminate, otherwise, jump to step 2.

A computer code in C++ was developed based on the above procedure. Before applying this code to the gain optimization of the multi-layered printed array, the accuracy of the code was first verified by applying it to the optimization of three well-known and challenging antenna problems: thinned phased array, Yagi-Uda array and aperiodic array [10,11]. These are, respectively, discrete, continuous and mixed parameter optimization problems. To the best knowledge of the PI, these efforts are the first applications of evolutionary programming in electromagnetics.

In the thinned phased array problem, the objective is to turn off some elements in a uniformly spaced or periodic array (with an inter-element spacing of one-half wavelength) to create a desired side-lobe level (SLL). For a  $2N$ -element symmetric array, thinning has  $2^{2N}$  possible combinations which is substantially large for large  $N$ . We applied EP to optimize a 200 element array for a SLL of -20 dB. The solution obtained for the 200 element array had 124 elements turned on and an SLL of -20.21 dB. The best solution in the Genetic Algorithm (GA) literature had 145 elements turned on [12], which has 17 percent more number of elements. For the case of a six element Yagi-Uda array, EP optimization with respect to the elements' lengths and inter-element spacings resulted in a directivity of 13.70 dBi which is comparable to the directivity of about 13 dBi reported in the literature using conventional optimization techniques.

## B. Implementation of EP for the Printed Yagi-Like Structure

To optimize the gain, the stacked printed dipole array is represented as a vector consisting of the length of the driver element, the director lengths, the dielectric constants, and the dielectric thickness as given below:

$$X = [x_{ref}, x_{dri}, x_{dir}(1) \dots x_{dir}(N-1), epr(1) \dots epr(N), dol(1) \dots dol(N)]^T \quad (5)$$

where  $x_{ref}$  and  $x_{dri}$  are the lengths of the reflector and driver, and  $x_{dir}(i)$ ,  $epr(i)$  and  $dol(i)$  are the length of the  $i$ -th director element in free-space wavelength,  $\lambda_0$ , the dielectric constant of  $i$ -th layer and the thickness of the  $i$ -th layer in dielectric wavelength,  $\lambda_{di}$ , respectively. In order to ensure that the optimized solutions obtained were practically feasible, the following constraints were chosen :

- a) Input resistance,  $R_{in}$ , should be larger than a minimum acceptable value.
- b) First-layer dielectric



thickness should be larger than a minimum value; for the microstrip version of the structure, a very thin substrate results in a very small bandwidth (alternatively, a requirement on the input impedance and/or gain bandwidths can be substituted for this constraint). c) Total thickness of the structure should be smaller than a maximum value in order to ensure a more compact and low profile design. The constraints were implemented by penalizing solutions that violated these constraints. The objective function (which is to be minimized) is then given by

$$\text{Fitness} = -\text{Gain dB} + P_a + P_b + P_c \quad (6)$$

where Gain dB is the gain in dBi obtained from the moment-method solution of the current distributions in MPIE in (1) and  $P_a$ ,  $P_b$  and  $P_c$  are the penalty criterion for violating the above constraints in (a), (b) and (c), respectively. In addition, limits were set on the maximum allowable values of each layer's dielectric constant and thickness during the optimization process as discussed below.

In the optimization process the driver length was set to its the resonance length (using a conventional quasi-Newton optimization scheme) in order to make the input impedance,  $Z_{in}$ , purely resistive, where as the  $x_{ref}$ ,  $x_{dir}(i)$ ,  $epr(i)$  and  $dol(i)$  were optimized using EP. A standard EP algorithm for continuous parameter optimization was applied as depicted in the flow-chart shown in Figure 17.

### C. Results and Discussions

A number of simulations for a 3-layer version of the microstrip structure in Figure 2 were performed. Four cases are reported here. For the first three cases dielectric constants were set fixed to  $\epsilon_{r1} = \epsilon_{r2} = \epsilon_{r3} = 2$  with constraints of minimum of  $0.1 \lambda_d$  for  $d_1$  and  $0.05 \lambda_d$  for  $d_2$  and  $d_3$ . Width of each strip element was  $w = 0.02 \lambda_0$ . For Case 1 the solutions were optimized without any constraints on  $R_{in}$  and the total thickness of the structure. High gains of 11 to 13 dBi and higher were quickly obtained within 35 generations (350 fitness evaluations). Table 1 shows the optimized parameters for a sample result obtained after only 10 generations. For this case a gain of 13.57 dBi is obtained with a radiation efficiency of 93%, which means a minimum amount of power is lost to the surface-waves. Due to the lack of constraint on the input resistance, however, a very low value of  $R_{in}$  is obtained. The current distributions for this case are plotted in Figure 18. The director 1 plays a major role in enhancing the gain as is evident from the magnitude of the current induced on its surface. Nevertheless as shown in table 2, presence of both directors is crucial in obtaining the optimum gain, an indication that the Yagi effect is at work..



Solutions in Case 2, were obtained subject to an additional constraint of  $R_{in} > 10$  ohms. This constraint causes a drastic increase in the number of generations. Gains of 10 to 11.5 dBi were obtained within about 140 generations. Optimized parameters resulted from the EP optimization after about 32 generations are listed in Table 1. Finally in Case 3, in addition to the above constraints, a constraint was also put on the maximum total thickness:  $D = d_1 + d_2 + d_3 < 0.5 \lambda_d$ . Within about 150 generations a high gain of about 9.88 dBi, with  $D = 0.447 \lambda_d$  (nearly  $0.316 \lambda_0$ ) was obtained. The corresponding current distributions are plotted in Figure 19. The constraint on  $R_{in}$ , forces the magnitude of the current on the feeder element to be less than those induced on the director elements. Removal of both directors in this case results in again of only about 4.30 dBi.

Table 1: Optimized 3-layer 'Yagi-like' stacked microstrip array

	Gain (dBi)	d1 ( $\lambda_d$ )	d2 ( $\lambda_d$ )	d3 ( $\lambda_d$ )	xdri ( $\lambda_0$ )	xdri(1) ( $\lambda_0$ )	xdri(2) ( $\lambda_0$ )	Rin ( $\Omega$ )	Rad. Eff. $\eta_s$
Case 1	13.57	0.240	0.120	0.360	0.3186	0.3180	0.3889	0.109	93 %
Case 2	11.10	0.299	0.252	0.491	0.2955	0.3005	0.3327	14.43	96 %
Case 3	9.88	0.125	0.092	0.230	0.2838	0.2881	0.3686	20.32	81 %
Case 4	15.66	0.192	0.299	0.258	0.3198	0.1583	0.4692	30.18	97 %

Table 2: Effects of director elements on gain in Case 1

	Both Directors present	Director 1 removed	Director 2 removed	Both Directors removed
Gain (dBi)	13.57	2.35	8.64	4.30

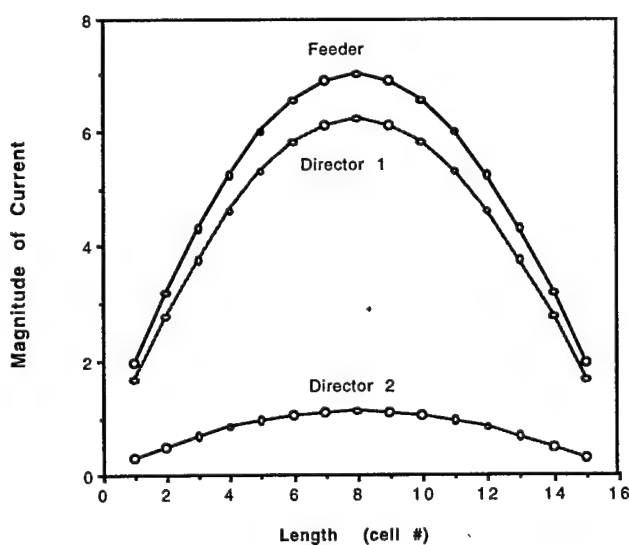


Figure 18: Current distributions for Case 1

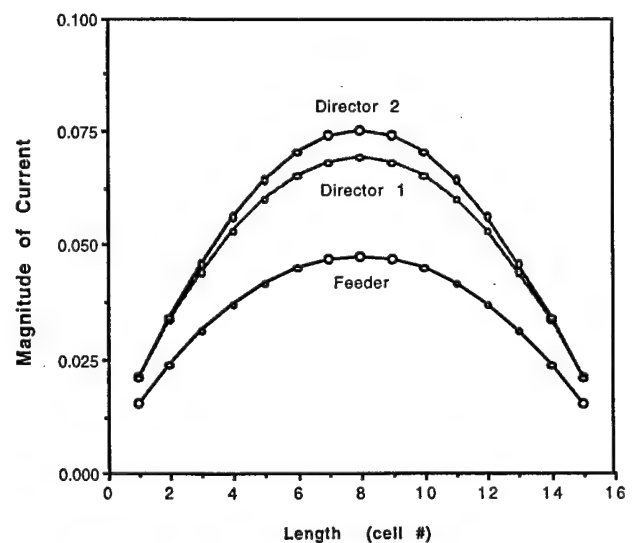


Figure 19: Current distributions for Case 3

Behavior of these three cases as a function of normalized frequency is shown in Figure 20. As can be seen, Case 1 with no constraints on  $R_{in}$  and  $D$  results in the highest gain at the expense of a very low gain bandwidth. Case 2 and 3 with a constraint on  $R_{in}$ , however, result in much higher bandwidths.

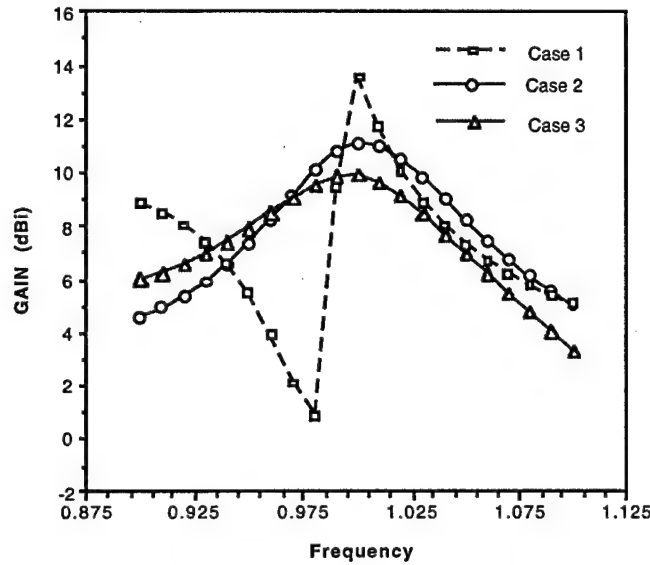


Figure 20: Gain of a printed 3-element stacked microstrip Yagi;  $\epsilon_{r1} = \epsilon_{r2} = \epsilon_{r3} = 2$ .

Finally in Case 4 the dielectric constants were allowed to vary in the range of 1.5 to 13 with a constraint of  $R_{in} > 10$  ohms. It was noted that  $\epsilon_{r1}$  and  $\epsilon_{r2}$  always tended to 1.5 while  $\epsilon_{r3}$  tended to 13; this is consistent with the high gain condition for an embedded dipole. A gain of 15.66 dBi and radiation efficiency of 97% were obtained with  $\epsilon_{r1} = \epsilon_{r2} = 1.5$  and  $\epsilon_{r3} = 11.23$  after 114 generations. The corresponding optimized parameters are shown in Table 1.

#### IV. FUTURE WORKS

Research works on the printed Yagi-like antennas that are either presently in progress or are planned for the 1998-1999 academic year include:

- Extension of the moment-method analysis of section II-B to the Yagi-like microstrip patch array, fed with a coaxial line ( see Figure 3).
- Theoretical investigation of Gain Enhancement methods for the Yagi-like antennas printed in a multi-layer anisotropic medium.

- Extension of the Evolutionary Programming technique of section III for gain optimization of a Yagi-like coaxial-fed patch array.
- Design, fabrication and measurement of an optimized Yagi-like coaxial-fed patch array.
- Investigation of other feed mechanisms for exciting the driver element. i.e., microstrip line, proximity-coupled line, etc.

In addition, a number of research tasks are planned for the topic-2 project, "New design concepts for low-profile dual-band CP microstrip antenna elements". Those tasks include:

- Development of design guidelines for the proposed dual frequency circularly-polarized electromagnetically fed microstrip antenna configurations.
- Characterization of the radiation parameters of each proposed configuration.
- Fabrication and experimental verification of selected design for operation in GPS and/or MSAT frequency bands.

## APPENDIX A

The mixed-potential Green's functions of a multi-layered microstrip structure, shown in Figure A.1, are of the Sommerfeld integral type which can be expressed as the inverse Bessel transformation,

$$G_{E,M}(z, \rho) = 2\pi \int_0^\infty \tilde{G}_{E,M}(z, \lambda) J_0(k_0 \rho \lambda) \lambda d\lambda \quad ; \quad \rho = \sqrt{(x-x')^2 + (y-y')^2} \quad (A.1)$$

where the spectral-domain Green's functions  $\tilde{G}_{E,M}(z, \lambda)$  satisfy the voltage distribution in the equivalent multi-section transmission line of Figure A.2,

$$\tilde{G}_{Ei} = \frac{1}{\lambda^2} (V_{mi} - V_{ei}) \quad ; \quad \tilde{G}_{Mi} = V_{mi} \quad (A.2)$$

The characteristic impedance in each section is given by:

$$Z_{ei} = (Z_{TM})_i = \frac{\gamma_i}{\omega \epsilon_{ri}} \quad , \quad \text{for } V_e \quad ; \quad Z_{mi} = (Z_{TE})_i = \frac{\omega \mu_{ri}}{\gamma_i} \quad , \quad \text{for } V_m$$

$$\gamma_i = -jk_0 \sqrt{\lambda^2 - \epsilon_{ri} \mu_{ri}}$$

where  $\gamma_i$  is the propagation constant in the  $i$ -th section of the line. In Figure A.2,  $Z_{gs}$  is the surface impedance of the ground-plane; for an structure without a ground-plane,  $Z_{gs}$  should be replaced by an open circuit representing the semi-infinite space.

To derive semi-analytical solutions for  $G$  we first extract out the static,  $1/k_0\rho$  singularity of  $G$ ; the remaining integral,  $g_r$ , is then divided into four regions as shown in Figure A.3: real-axis regions from 0 to  $\lambda_s (= 1 - \delta_1)$ ,  $\lambda_e (= n_{\max} - \delta_2)$  to some  $\lambda_{\max} (>> 1)$  and  $\lambda_{\max}$  to infinity, and the complex-contour region between  $\lambda_s$  and  $\lambda_e$ . Here  $n_{\max}$  is to the largest refractive index of the dielectric layers, and  $\delta_1$  and  $\delta_2$  are chosen as some arbitrary small, but not very close to zero, positive values. We note that this contour avoids any possible surface-wave poles, located on the real axis in the region  $1 < \lambda < n_{\max}$ . Cubic-spline interpolations are used to curve-fit the integrand,  $\tilde{G}$ , in each region, except in the  $\lambda_{\max}$  to infinity region for which the integration range is divided into small pieces, using an adaptive marching scheme, and  $\tilde{G}$  is approximated on each piece by the first few terms in it's Taylor-series expansion in  $\lambda^{-2}$ . Care should be exercised, however, in selecting the height of the deformed contour,  $h$ , above the surface-wave poles in order to ensure

the smoothness of the integrand,  $\tilde{G}$ , in (A.1) before applying the cubic-spline interpolation. Numerical experimentation of various structures show that accurate results for the deformed part of the contour can be obtained by selecting the height  $h$  in Figure A.3 as  $\text{Min}(0.2, 2/k_0\rho_{\max}) < h < \text{Max}(0.8, 2/k_0\rho_{\max})$  in the cubic-spline interpolation.

Once the curve-fit as well as the Taylor-series coefficients are determined, the resulting integrals of the type,

$$Q_m = \int \lambda^m J_0(k_0\rho\lambda) d\lambda, \quad m = -4, -2, 0, 1, 2, 3, \dots \quad (\text{A.3})$$

can be expressed in closed forms in terms of Bessel and Struve functions. For the first two real-axis regions, the final expression for  $g_r(\rho)$  is of the form [14],

$$g_r(\rho) = \sum_{n=1}^{N+1} \left\{ \frac{(A_n - A_{n-1})}{k_0\rho} Q_0(k_0\rho\lambda_n) + \frac{(B_n - B_{n-1})}{(k_0\rho)^2} Q_{+1}(k_0\rho\lambda_n) + \frac{(C_n - C_{n-1})}{(k_0\rho)^3} Q_{+2}(k_0\rho\lambda_n) + \frac{(D_n - D_{n-1})}{(k_0\rho)^4} Q_{+3}(k_0\rho\lambda_n) \right\} \quad (\text{A.4})$$

where  $A_n$ ,  $B_n$  and  $C_n$  are functions of the cubic-spline coefficients, and

$$\begin{aligned} Q_0(x) &= 1 - x J_0(x) + \frac{\pi x}{2} [J_0(x) \mathbf{H}_1(x) - J_1(x) \mathbf{H}_0(x)] \quad ; \quad Q_{+1}(x) = x J_1(x) \\ Q_{+2}(x) &= Q_0(x) + x J_0(x) + x^2 J_1(x) \quad ; \quad Q_{+3}(x) = 2x^2 J_0(x) - x(x^2 - 4) J_1(x) \end{aligned} \quad (\text{A.5})$$

wherein  $J_i$  and  $\mathbf{H}_i$  are the Bessel and Struve functions [13], respectively. The expression for the  $\lambda_{\max}$  to infinity region is similar to (A.4) but in terms of  $Q_0$ ,  $Q_{-2}$  and  $Q_{-4}$  [14].

We note that  $Q_m$  expressions are functions of distance  $\rho$  only and independent of the dielectric layers' thickness and material properties. Therefore, once the constants in the cubic-spline interpolations and Taylor-series expansions are computed and stored, the Sommerfeld integral can be evaluated for all values of  $\rho$  at once, resulting in a substantial reduction in the CPU time. Additional CPU time saving can also be achieved for the first three regions of the contour if one notes that the  $Q_m$  functions in (4) need to be computed only once for a given set of  $k_0\rho$  values, stored and then used for all  $M$  Green's functions of an  $N$ -layer structure.

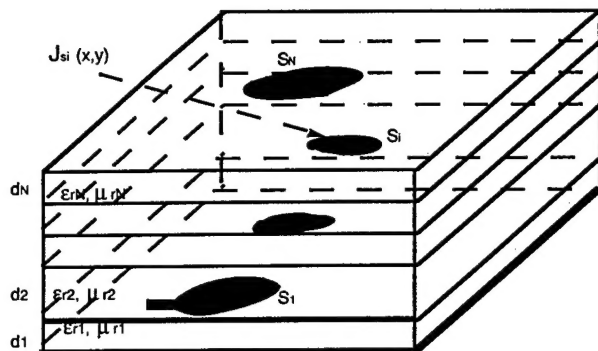


Figure A.1: A multilayer microstrip structure

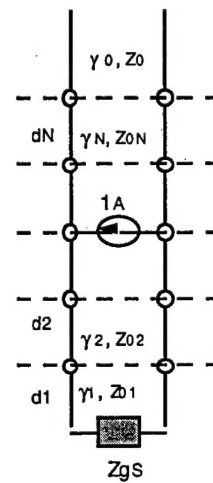


Figure A.2: The equivalent transmission-line model

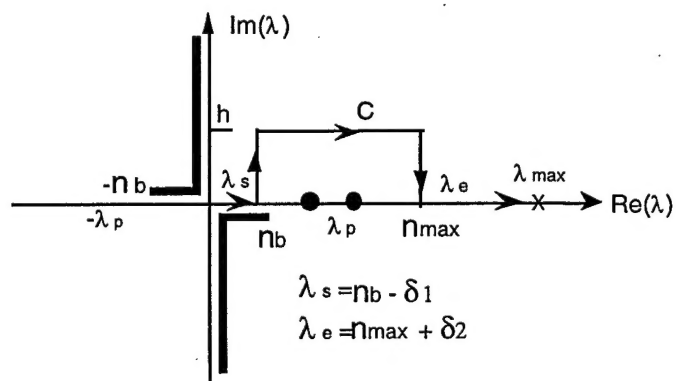


Figure A.3: Contour of integration for a multi-layered structure



## REFERENCES

- [1] D. R. Jackson and N. G. Alexopoulos, "Gain enhancement methods for printed circuit antennas", *IEEE Trans. Antennas Propagat.*, Vol. AP-33, pp. 976-987, Sept. 1985.
- [2] H. Y. Yang and N. G., Alexopoulos, "Gain Enhancement technique for microstrip antennas," *IEEE Trans. Antennas Propagat.*, Vol. AP-35, pp. 860-863, July 1987.
- [3] J. R. Mosig, "Arbitrary shaped microstrip structures and their analysis with a mixed potential integral equation," *IEEE Trans. on Microwave Theory Tech.*, MTT-36, pp. 314-323, February 1988.
- [4] A. Hoorfar, J. X. Zheng and D. C. Chang, "Numerical modeling of cross-over and other Junction discontinuities in two-layer microstrip circuits," *Int. Journal of Microwave and Millimeter-wave Computer-Aided Eng.* Vol. 2, No. 4 , pp. 261-272, October 1992.
- [5] J. R. Mosig and E. F. Gardiol, "A dynamical radiation model for microstrip structures", *Advances in Electronics and Electron Physics*, P. Hawks, Ed. Vol. 59, Academic Press, , pp. 139-237, 1992.
- [6] A. Hoorfar, "Analysis of a 'Yagi-Like' printed stacked dipole array for high gain applications," *Microwave Opt.. Technol. Lett.*, pp. 317-321, April 1998.
- [7] D. E. Goldberg, *Genetic algorithms in search, optimization and machine learning*, Reading, MA: *Addison Wesley*, 1989.
- [8] D. B. Fogel, *Evolutionary Computation: Toward a New Philosophy of Machine Intelligence*, Piscataway, NJ: *IEEE Press*, 1994.
- [9] J. M. Johnson and Y. Rahmat-Samii, "Genetic algorithms in engineering electromagnetics," *AP-S Magazine*, vol. 39, pp. 7-25, August, 1997.
- [10] K. Chellapilla, S.S. Rao and A. Hoorfar, "Optimization of thinned phased arrays using evolutionary programming," *EP 98 : Proc. of the Seventh Intl. Conf. on Evolutionary Programming*, Springer-Verlag: New York, March 1998.
- [11] K. Chellapilla and A. Hoorfar, " Evolutionary programming: an efficient alternative to genetic algorithms for electromagnetic optimization problems," *Proceedings of the IEEE AP-S International Symposium*, Atlanta, GA, pp. 42-45 , June 1998.
- [12] R. L. Haupt, "Thinned Arrays Using Genetic Algorithms," *IEEE Trans. on Antennas and Propagation*, vol. 42, no. 7, July 1994.
- [13] Abramowitz, M. and A. Stegun, Handbook of Mathematical Functions, Dover Publication, Inc., New York, 1970.
- [14] A. Hoorfar and D. C. Chang, "Semi-analytical solutions for microstrip Green's functions in multi-layered media," *Proceedings of the 1998 International Symposium on Electromagnetic Theory* , PP. 618-620, May 1998, Thessaloniki, Greece.

REPORT DOCUMENTATION PAGE			Form Approved OMB No. 0704-0188	
Public reporting burden for this collection of information is estimated to average 1 hour per response, including the time for reviewing instructions, searching existing data sources, gathering and maintaining the data needed, and completing and reviewing the collection of information. Send comments regarding this burden estimate or any other aspect of this collection of information, including suggestions for reducing this burden to Washington Headquarters Services, Directorate for Information Operations and Reports, 1215 Jefferson Davis Highway, Suite 1204, Arlington, VA 22202-4302, and to the Office of Management and Budget, Paperwork Reduction Project (0704-0188), Washington, DC 20503.				
1. AGENCY USE ONLY (Leave blank)		2. REPORT DATE October 12, 1998		3. REPORT TYPE AND DATES COVERED Interim: October 15th, 1997 - September 30th, 1998
4. TITLE AND SUBTITLE INVESTIGATION OF A NEW CLASS OF LOW-PROFILE MULTI-LAYER PRINTED ANTENNAS			5. FUNDING NUMBERS  G - N00014-98-1-0090	
6. AUTHOR(S)  Ahmad Hoorfar				
7. PERFORMING ORGANIZATION NAMES(S) AND ADDRESS(ES)  Villanova University 800 Lancaster Ave. Villanova, PA 19085			8. PERFORMING ORGANIZATION REPORT NUMBER  Acc: 527615	
9. SPONSORING / MONITORING AGENCY NAMES(S) AND ADDRESS(ES)  Office of Naval Research Ballston Center Tower One 800 North Quincy Street Arlington VA 22217-5660			10. SPONSORING / MONITORING AGENCY REPORT NUMBER	
11. SUPPLEMENTARY NOTES				
a. DISTRIBUTION / AVAILABILITY STATEMENT  Approved for Public Release: distribution is unlimited			12. DISTRIBUTION CODE	
13. ABSTRACT (Maximum 200 words)  This progress report outlines our research efforts on modeling, analyses and optimization of a novel class of multi-layered printed antennas for high gain applications. The proposed antennas, which are based on a multi-layer printed-circuit version of the conventional Yagi array, are very attractive for applications that require high gain antennas in a compact low-profile package. Presence of the dielectric layers not only hinders the need for structural support of the antenna but also provides a few more degrees of freedom for gain optimization. In addition, these antennas can be made conformal to various shapes and surfaces. Our research during this interim period has resulted in three contributions: 1) We have developed a numerical code for efficient electromagnetic modeling of these Yagi-like structures. A novel feature of this code is a new semi-analytical technique that speeds up the evaluation of the corresponding Green's functions by a factor of 10 or higher. 2) The feasibility of obtaining high gain from the proposed Yagi-like arrays is investigated by performing a detailed parametric study for structures with up to 5 dielectric layers. 3) We have developed an electromagnetic optimization engine based on Evolutionary Programming. This code is applied to optimal design of the printed Yagi-like arrays. Optimization is performed with respect to lengths of driver and director elements as well as dielectric constants and thickness of layers under different constraints' criteria. It is shown that a globally optimized three layer structures can achieve a gain of 13 dBi or higher without the need for high permittivity dielectric layers.				
14. SUBJECT TERMS  Printed Yagi-Like arrays, Multi-Layered Microstrip Antennas, Method of Moments, Gain Optimization, Evolutionary Programming			15. NUMBER OF PAGES 26	
			16. PRICE CODE	
17. SECURITY CLASSIFICATION OF REPORT UNCLASSIFIED	18. SECURITY CLASSIFICATION OF THIS PAGE UNCLASSIFIED	19. SECURITY CLASSIFICATION OF ABSTRACT UNCLASSIFIED	20. LIMITATION OF ABSTRACT	